Aeolian Research 3 (2011) 55–66

Contents lists available at ScienceDirect

Aeolian Research

journal homepage: www.elsevier.com/locate/aeolia

The association of land cover with aeolian sediment production at Jornada Basin, New Mexico, USA

Kevin W. Floyd [a], Thomas E. Gill [a,b,*]

[a] Environmental Science and Engineering Program, University of Texas at El Paso, El Paso, TX 79968, USA
[b] Department of Geological Sciences, University of Texas at El Paso, El Paso, TX 79968, USA

ARTICLE INFO

Article history:
Received 16 May 2010
Revised 23 November 2010
Accepted 4 February 2011
Available online 10 March 2011

Keywords:
Land cover
Chihuahuan Desert
Dust flux
Vegetation communities
Sand transport
Particle size

ABSTRACT

We investigated amounts and particle size distributions (PSDs) of aeolian sediments collected at five heights in five ecosystem types at the Jornada Basin, Chihuahuan Desert, New Mexico, USA. Particle size distributions, mass fluxes, and percent of dust-sized (⩽50 μm) mass flux were determined for all heights and all ecosystem types. Differences between sites were determined using ANOVA followed by Tukey–Kramer post hoc tests to find groupings. For creosote shrublands, grasslands, and two tarbush-dominated alluvial flats, samples collected at 5, 10, and 20 cm had >80% sand-sized (>50 μm) particles, while one playa and tarbush site yielded ~45% dust-sized particles at 5 and 10 cm. The transition from saltation to suspension was ~20 cm for most sites. Two mesquite dune sites and an anthropogenically devegetated site, all with high overall mass fluxes, shifted to suspension at ~50 cm. Highest dust fluxes occurred at the devegetated site, followed by the playa, a mesquite site with unvegetated "streets," and tarbush sites. These field observations are consistent with laboratory-based dust emission experiments and remote sensing studies in the Chihuahuan Desert. Playas and tarbush sites are major dust producers due to high proportions of fines, whereas the mesquite site produces much dust because of greater overall mass flux. Mesquite dunes covering most of the basin likely produce the most dust overall, though playas and tarbush-dominated alluvial flats (which cover about 8%) can emit large amounts of dust. Continuing shrubland encroachment will likely increase dust emissions from the Jornada Basin, as well as in other arid regions.

1. Introduction

The expansion of woody plants, typically into semiarid and mesic grasslands, has been documented in both North and South America, southern Africa, Australia, Asia, and Europe (e.g., Altesor et al., 2006; Angassa, 2005; Archer et al., 1988; Cabral et al., 2003; Cheng et al., 2004; Costello et al., 2000; Kraaij and Milton, 2006; Peters and Gibbens, 2006; Scholes and Archer, 1997; Van Auken, 2000). Conversion from grasslands to woody plant-dominated landscapes has important local, regional, and global consequences, including changes in carbon dynamics, loss of biodiversity and forage production, changes in hydrological budgets, and wind and water erosion of soil and nutrients (Peters et al., 2006; Safriel and Adeel, 2005).

The type and amount of vegetation cover is an important factor in determining wind erosion. Although models differ in what aspect of vegetation cover is most important (such as total cover versus lateral cover), there is general agreement that shrublands provide less protection from wind erosion than grasslands (e.g., Hesse and Simpson, 2006; Okin et al., 2006). Redistribution of soil material by wind occurs from the local scale (from the interspace to under shrubs), the patch scale (dust removed for long-distance transport), and the global scale (deposition of nutrients in downwind ecosystems) (Okin et al., 2006). The size of the eroded particle will determine its transport mechanism, with larger particles more likely to be transported relatively short distances via saltation, while smaller particles can be transported larger distances via suspension. Saltating particles are more likely to influence local processes, while suspended particles are more likely to influence regional to global processes. The transition between saltation-dominated and suspension-dominated transport depends upon surface conditions and wind velocity, and is often found ~20–30 cm above the surface for dryland soils (Fryrear and Saleh, 1993). In locations with low surface cover and/or high wind velocities, the larger particles can be lifted higher above the surface, increasing the height of the transition layer (Warren et al., 2007). Thus, understanding how types of and changes in land cover impact aeolian processes is critical for both local and global systems, understanding past processes, and predicting future changes in aeolian processes as climatic change leads to ecosystem changes (Reynolds et al., 2003). Landscape characteristics – including both geomorphology and vegetation type and cover – modulate

* Corresponding author at: Department of Geological Sciences, University of Texas at El Paso, El Paso, TX 79968, USA. Tel.: +1 915 747 5168; fax: +1 915 747 5073.
E-mail address: tegill@utep.edu (T.E. Gill).

1875-9637/$ - see front matter © 2011 Elsevier B.V. All rights reserved.
doi:10.1016/j.aeolia.2011.02.002

the location as well as the intensity of wind erosion. Playas (dry lake beds in topographically closed desert basins) have long been considered to be primary "hotspots" of dust emission (Engelstaedter et al., 2003; Gill, 1996; Ginoux et al., 2001; Prospero et al., 2002; Reynolds et al., 2007) to the point that the distribution of topographic lows in drylands has been used as a proxy for source areas in models of long-distance transport of dust (Ginoux et al., 2004; Mahowald et al., 2002; Zender et al., 2003). In an analysis of global dust storm frequency (DSF) records, Engelstaedter et al. (2003) suggested that DSF is highest in bare ground areas and increases as the fraction of closed topographic depressions increases. DSF in shrublands was found to be ~1/3 that of topographic depressions yet an order of magnitude higher than in grasslands (Engelstaedter et al., 2003). In the Mojave Desert/Southern Great Basin of North America, Reheis and Kihl (1995) found that playas and alluvial sources produce roughly equivalent amounts of dust per unit area, although total dust production from the more spatially extensive alluvial sources is much larger.

Vegetation protects soils from wind erosion through three primary mechanisms: (1) providing direct shelter from the force of wind by covering a fraction of the surface and creating a lee-side wake where wind speeds are dramatically reduced, (2) extracting momentum from the wind, thus reducing erosivity, and (3) trapping windborne particles, reducing total flux and providing a loci for sediment deposition (Okin et al., 2006; Wolfe and Nickling, 1993). Many modeling efforts have shown that three aspects of vegetation are important predictors of wind erosion: (1) percent cover, which is related to simple surface protection, (2) lateral cover (the total frontal silhouette area of vegetation intercepted by wind), which affects how much momentum the vegetation can extract from the wind, and (3) the spatial distribution of the vegetation, which impacts the fetch distance (Li et al., 2007; Okin et al., 2009, 2006; Wolfe and Nickling, 1993). The longer the fetch distance, the more aeolian sediment flux occurs. Desert grasslands tend to have greater overall cover, greater lateral cover, and shorter aeolian fetch distances than do shrublands (Gillette and Monger, 2006), all characteristics that should reduce aeolian erosion from grasslands compared to shrublands.

Blowing dust and sand is frequent in the Chihuahuan Desert (CD) of southwestern North America (Bowker et al., 2008), making it one of the aeolian hotspots of the continent (Prospero et al., 2002). Shrublands are the predominant land cover type of the CD, especially the uplands, while grasslands are the typical lowland vegetation of the desert (Beltrán-Przekurat et al., 2008; Gibbens et al., 2005), and playas of varying size are scattered throughout. Remote-sensing-based analyses of regional dust events throughout the Chihuahuan Desert have suggested that shrublands are the most important dust source areas overall and grasslands are relatively minor contributors (Rivera Rivera et al., 2010), although playas/unvegetated lands are clearly also major dust sources (Rivera Rivera et al., 2010) and dominate some individual events within the CD (Dominguez Acosta, 2009; Gill et al., 2009; Lee et al., 2009).

The Jornada Long Term Ecological Research site (LTER), located in the northern CD of south-central New Mexico, USA, has been the site for several studies on aeolian processes in arid environments (Belnap and Gillette, 1998; Bergametti and Gillette, 2010; Gillette and Monger, 2006; Gillette and Chen, 2001; Gillette et al., 2006; Gillette and Pitchford, 2004; Okin and Gillette, 2001). Much of the work has compared emissions from bare surfaces with those from areas dominated by mesquite (*Prosopis grandulosa*) shrubs. Okin and Gillette (2001) found areas of extremely long aeolian fetch distance (termed "streets") tending to be aligned with the direction of the prevailing wind in some mesquite (*Prosopis* sp.)-dominated shrublands (but not reported in the literature from other types of shrublands in the CD or elsewhere). The faster wind flow down these "streets" (Bowker et al., 2006) makes them the dominant local sources of wind-eroding sand (Bowker et al., 2008) Mesquite-dominated areas in the Jornada LTER were shown by Gillette and Pitchford (2004) to have roughly 10 times the amount of aeolian sand flux as areas with other vegetation types. The flux was greatest at the end of the "streets" in-between mesquite patches, while sediment collectors placed just downwind of mesquite bushes had less flux (Gillette and Pitchford, 2004). This demonstrates the importance of spatial distribution of vegetation, as flux in mesquite areas was not well explained by simply describing the vegetation coverage.

Less work has been done investigating the effects that different vegetation types have on aeolian processes (although see Gillette and Pitchford, 2004). The five most common vegetative types in the Jornada LTER are honey mesquite (*Prosopis grandulosa*) dune shrublands, black grama (*Bouteloua eriopoda*) grasslands, creosote bush (*Larrea tridentata*) shrublands, tarbush (*Flourensia cernua*) shrublands on alluvial flats, and grass-dominated (characterized by *Pleuraphis mutica*) playas (Huenneke et al., 2001, 2002; Peters and Gibbens, 2006). The Jornada LTER has experienced major changes in its plant communities over the past 100 years (Gibbens et al., 2005; Peters and Gibbens, 2006). Black grama grasslands have decreased from covering about 19% of the Jornada in 1915–1916 to only about 8% in 1998 (Gibbens et al., 2005). Honey mesquite increased from covering about 26% of the Jornada to 59% total coverage in 1998, with 27% classified as mesquite dunes (soil accumulations at the base of plants 20 cm to about 3 m in height) and 17% as mesquite sandhills (accumulations greater than 3 m in height) (Gibbens et al., 2005).

Three study sites in each of these vegetative types were established in 1989 to study net primary productivity (NPP) and vegetation change (Huenneke et al., 2002). Bergametti and Gillette (2010) found significantly higher horizontal mass flux at mesquite sites from 1998 to 2005 than at each of the other four vegetation types. The mass fluxes at the other four vegetation types (grasslands, creosote bush, tarbush, and playa) were statistically indistinguishable from each other. Saltation was determined to be the mechanism for flux at the mesquite sites, but did not explain the flux patterns at the other vegetation sites. Size distributions of the transported particles were not examined by Bergametti and Gillette (2010) nor in previous studies of aeolian processes at the Jornada LTER.

In this study, we investigate the amounts and particle size distributions (PSDs) of material collected in Big Spring Number Eight (BSNE) aeolian sediment samplers (Fryrear, 1986) in late spring–early summer (the windy season) 2006 near each of the NPP sites in the five vegetative types the Jornada LTER. We also estimate amount of silt- and clay-sized particles ($\leqslant$50 μm, "dust") produced at these different sites. The mesquite-dominated regions have been shown to experience more aeolian mass flux than other vegetation types (Bergametti and Gillette, 2010; Gillette and Monger, 2006; Gillette and Pitchford, 2004), and understanding the characteristics of particle size composition of aeolian erosion from within these different vegetation types will be important as mesquite and creosote continue to replace historical grasslands at the Jornada and other sites in the Chihuahuan Desert, and as woody shrubs replace grasslands worldwide.

2. Methods

2.1. Sample collection

Detailed descriptions of sample collection can be found in Bergametti and Gillette (2010). Briefly, Big Spring Number Eight (BSNE) aeolian sediment samplers (Fryrear, 1986) were deployed at sites adjacent to the 15 NPP sites described above (see Bergametti and Gillette (2010), for a map of the study sites). There are three sites

per vegetative type (mesquite, grama grassland, creosote, tarbush, and playa), and each site is named with the initial of the vegetation site and a four letter code representative of the site (i.e., P-TOBO is a playa site with Tobosa grass present, Table 1). The non-mesquite sites had four sampler towers, each located at the corners of a 10 m square. Three sites had incomplete sampling at one of the four towers, generally caused by problems with one or more of the BSNE samplers, but we analyzed the samples collected from the remaining three towers (Table 1). For the mesquite sites, one (M-NORT) had a dense sampling design with 10 BSNE towers, detailed by Gillette et al. (2006). The other two mesquite sites (M-WELL and M-RABB) had single sampling towers. Each tower had five BSNE samplers, with the mouths of the samplers set at 5, 10, 20, 50, and 100 cm above the soil surface. Where multiple sampling towers existed and collected enough sediment for analysis, we analyzed samples from all towers and report the average results with error bars representing one standard deviation. The BSNE samplers at two of the three playa sites (P-COLL and P-SMAL) did not collect enough aeolian sediment for analysis of particle size distribution, and thus are not included in the analysis. The particle size distributions for M-WELL and M-RABB were determined, but because of the lack of replicate sampling towers, those results were not included in the statistical analysis described below. However, earlier work has shown that M-WELL, with a more homogeneous distribution of mesquite plants and lack of well-developed "streets," has less aeolian mass flux than the other two mesquite sites (Bergametti and Gillette, 2010; Okin and Gillette, 2001). Thus we wanted to determine if there were differences in the particle size distributions and mass flux of dust-sized particles for the different mesquite sites. An artificially devegetated site, designated "SCRAPE" by Gillette and Chen (2001), was sampled with three BSNE towers to show the effect of the devegetation on aeolian sediment flux. The length of time each site was sampled varied, but the samples analyzed in this study were all collected during spring, which is the windiest season in the Jornada Basin (Bergametti and Gillette, 2010; Wainwright, 2006), and early summer of 2006 (Table 1).

2.2. Particle size analysis

Sediment samples from the BSNEs were dried and weighed, and daily horizontal mass flux was calculated by dividing the mass of the collected sediment by the area of the BSNE orifice and by the number of days the sampler was deployed. This standardizes the mass of the collected sediment by the size of the BSNE sampler mouth and the amount of time of sample collection. BSNE samplers have been shown to have collection efficiencies of close to 90% for airborne soil particles >50 μm in diameter (Shao et al., 1993), but only around 30–40% for particles ⩽50 μm in diameter (Goossens and Offer, 2000; Shao et al., 1993). Thus the measured particle size distributions likely underrepresent the amount of dust-sized (⩽50 μm) particles. Prior to analysis, vegetative debris and particles >2 mm were removed by hand as thoroughly as possible. This sorting did break up some of the dry sediment aggregates present in some of the samples, particularly those from T-WEST and P-TOBO.

Volumetric particle size distributions were measured with a Malvern Mastersizer 2000 laser diffractometer (Malvern Instruments Ltd., Worcestershire, UK), using the Scirocco 2000 accessory for sample dispersion in air and the Hydro 2000 accessory for sample dispersion in water, generally following the protocols recommended by Sperazza et al. (2004) and Zobeck (2004). Samples dispersed in water were not treated with a chemical dispersant prior to analysis, but were sonicated for 30 s prior to particle size measurements to help uniformly disperse the particles. Dry dispersion requires more sample than does the dispersion in water, so small samples (typically <0.5 g) were analyzed wet while larger samples (>1.0 g) were analyzed dry. Samples from the mesquite sites, the SCRAPE site, and some of the grassland sites were analyzed dispersed in air (110 samples total), while samples from the remaining sites were analyzed dispersed in water (152 samples total). A subset of samples was analyzed both dry and wet, with both methods of dispersal giving very similar results for sandy sediments (Fig. 1). For the two sites with higher percentages of clay- and silt-sized particles (T-WEST and P-TOBO), the dispersal in water gave qualitatively similar results, but with the median particle size shifted toward finer particles (Fig. 1). For these sites, we used the particle size distributions obtained using wet dispersion for data analysis. Replicate aliquots of samples were analyzed when sufficient sediment was collected, and these replicates also had very similar PSDs (data not shown). When replicate aliquots were analyzed, we averaged the PSDs for data analysis.

To assess the shape of the particle size distribution, the Malvern proprietary software was used to calculate the median particle size

Table 1
Description of sample locations, soil texture, percentages of clay-, silt-, and sand-sized particles present in the ⩽2 mm size fraction, and sampling dates.

Vegetation type	Site name	Latitude[a]	Longitude[a]	Soil texture[a]	% Clay[a]	% Silt[a]	% Sand[a]	# BSNE sampling towers	Sampling start date	Sampling end date
Creosote	C-CALI	32.5136	−106.7961	Sandy loam	8.3	17.1	74.6	4	4/13/2006	7/4/2006
	C-GRAV	32.4892	−106.7817	Sandy loam	7.7	12.5	79.8	4	4/13/2006	7/4/2006
	C-SAND	32.5144	−106.7906	Coarse sandy loam	8.7	15.9	75.4	4	4/13/2006	7/4/2006
Grassland	G-BASN	32.5297	−106.7856	Loam	21.6	20	58.4	3	6/9/2006	7/4/2006
	G-IBPE	32.5886	−106.8436	Loamy fine sand	6.8	8.6	84.6	4	4/13/2006	7/4/2006
	G-SUMM	32.5144	−106.8003	Loamy sand	6.9	14.1	79	4	4/13/2006	7/4/2006
Tarbush	T-EAST	32.5136	−106.7401	Sandy loam	11	26.4	62.6	3	4/12/2006	6/9/2006
	T-TAYL	32.5469	−106.7106	Sandy clay loam	20.7	23.9	55.4	3	4/12/2006	6/9/2006
	T-WEST	32.5127	−106.7430	Sandy clay loam	17.9	31.1	51	4	4/13/2006	7/4/2006
Playa grassland	P-TOBO	32.6678	−106.7719	Clay loam	35.5	30.4	34.1	4	4/13/2006	7/4/2006
Mesquite	M-NORT	32.6186	−106.7858	Loamy fine sand	7.9	3.1	89	10	11/30/2005	5/22/2006
	M-RABB	32.6103	−106.7964	Loamy fine sand	8	6.4	85.6	1	11/30/2005	5/22/2006
	M-WELL	32.6047	−106.8508	Loamy fine sand	6.3	5.4	88.3	1	11/30/2005	5/22/2006
Devegetated	SCRAPE	32.5390[b]	−106.7583[b]	Loamy sand[b]	na	na	na	3	6/1/2006	6/23/2006

[a] Data from National Soil Survey Center, USDA-NRCS, Lincoln, NE.
[b] Data from Gillette and Chen (2001).

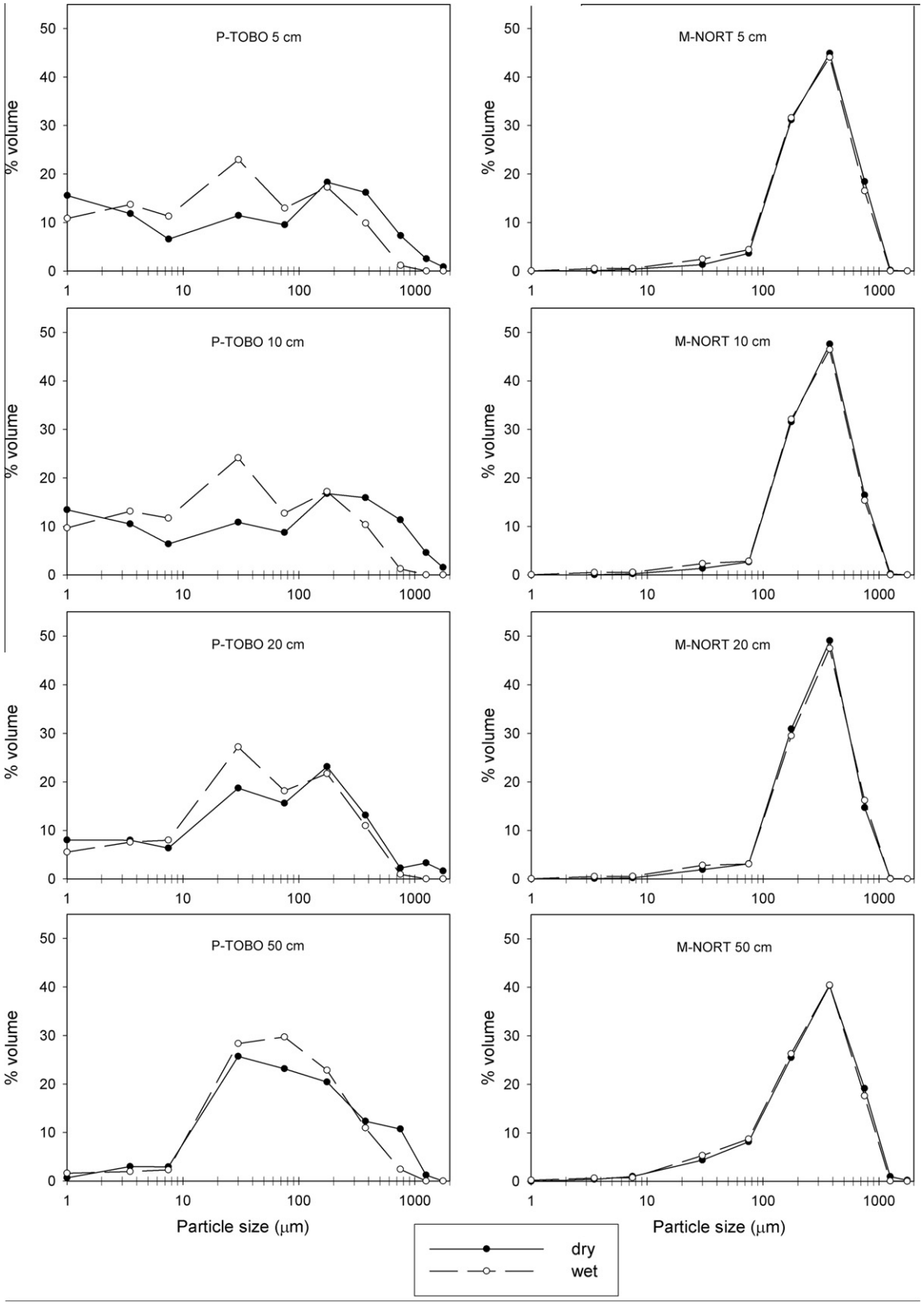

Fig. 1. Comparison of particle size distributions obtained using samples dispersed in water and samples dispersed in air. For the samples from 5 and 10 cm from the second tower at the playa site P-TOBO, dispersal in water shows a slight shift towards finer particles, although the overall particle size distributions are qualitatively similar. As the height at which the sample was collected increases, the results from both types of dispersal are very similar. For the samples collected at tower *D*6.5 at the mesquite site M-NORT, there is no discernable difference in the particle size distributions with either dispersal method.

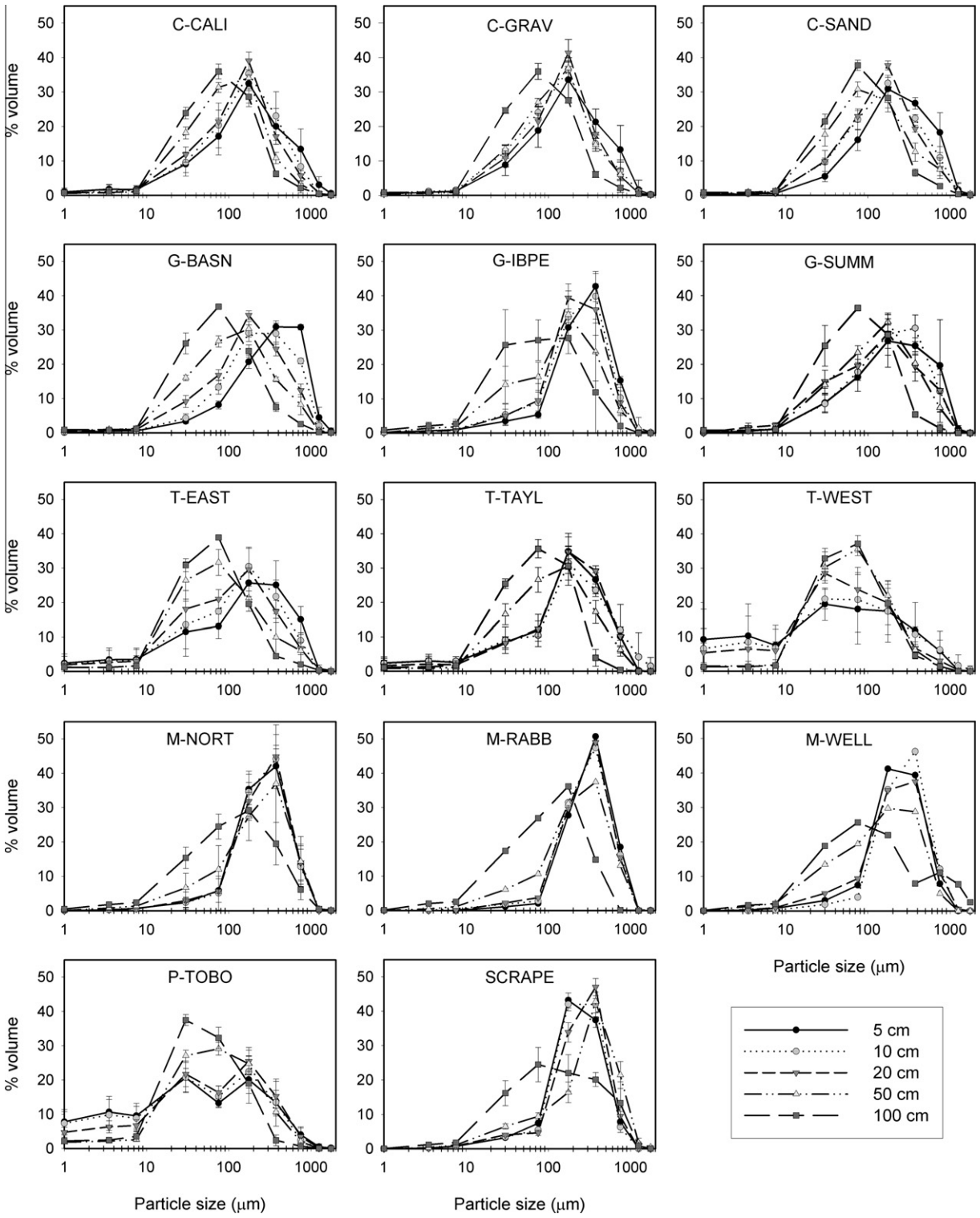

Fig. 2. Particle size distributions of BSNE-collected sediments at 5, 10, 20, 50, and 100 cm above the soil surface for each site. For most sites, the sediments from the 5, 10, and 20 cm heights have very similar PSDs, dominated by sands. The sediments from the 50 and 100 cm heights shift towards finer particles. Sites P-TOBO and T-WEST have larger percentages of dust ($\leqslant$50 μm) at the lower heights.

and the span of the particle size distribution. The span is calculated as the diameter at which 90% of the particle size distribution falls below ($D(0.9)$) minus the diameter at which 10% of the particle size distribution falls below ($D(0.1)$), divided by the median particle size ($D(0.5)$). Span is similar to kurtosis (a measure of how peaked or flat the distribution is), and, combined with the median particle size, gives a quantitative method of comparing particle size distributions. The percent of particle volume in different size classes was also measured, including the percent of the sample in the dust size range (defined here as $\leqslant$50 μm diameter). The production of dust-sized particles was estimated by multiplying the percentage of sample in that size category by the horizontal mass flux for each

location and height. The transition between saltation (coarser particle)-dominated transport and suspension (finer particle)-dominated transport (Fryrear and Saleh, 1993) was determined by finding the height at which the PSDs changed from the distributions seen at 5 and 10 cm above the soil surface to the distributions seen at higher heights.

2.3. Statistical analysis

The median particle size, span of the particle size distribution, horizontal mass flux, and the estimated mass of dust-sized particles produced at the different sites were log-transformed for normality as needed and compared for each height using one-way ANOVA. If the ANOVA was significant, the means were compared using the Tukey–Kramer test. All statistics were calculated using JMP 8.0 (SAS Institute, Cary, NC).

3. Results

3.1. Particle size distributions

3.1.1. Particle size distributions at each site

At the lower heights (5 and 10 cm), all sites except the playa site (P-TOBO) and one tarbush site (T-WEST) had >80% sand-sized particles (>50 μm), as would be expected within the saltation zone, with median particle sizes of 180–380 μm (Supplementary Fig. 2). Samples from the 20 cm height from all of the creosote sites, two of the grassland sites (G-BASN and G-IBPE), one mesquite site (M-WELL), and the other two tarbush sites (T-TAYL and T-EAST) were all similar to those from 5 and 10 cm. The sediments at 50 and 100 cm shifted progressively finer, with median sizes of 80–130 μm at 50 cm and 60–80 μm at 100 cm (Fig. 2). The similarities of the PSDs at 5, 10, and 20 cm combined with the shift to finer particles at 50 and 100 cm suggest that the transition from saltation (coarser particle, sand)-dominated transport to suspension (finer particle, dust)-dominated transport (Fryrear and Saleh, 1993) occurs between 20 and 50 cm.

The exceptions to these patterns were the one playa site (P-TOBO) and one tarbush site (T-WEST), where approximately 45% of the sediment at 5 and 10 cm was silt- and clay-sized particles (⩽50 μm), and the median particle sizes were approximately 60 μm (Fig. 2). The PSDs for sediments at 50 and 100 cm heights above the playa site were similar to each other, with fewer ⩽10 μm particles than at 5 and 10 cm, but with more 10–50 μm particles than at lower heights. The PSD for sediments at 20 cm was similar to the sediments from 5 and 10 cm, although with fewer ⩽10 μm particles. A similar pattern was seen at the tarbush site (T-WEST), with the 20 cm sample having more 10–50 μm particles but fewer coarse sand (>500 μm) particles than at 5 and 10 cm (Fig. 2). Although the sediments at the lower heights (5, 10, and 20 cm) were finer than those at the upper heights, the change in PSDs with height suggests the transition between saltation-dominated and suspension-dominated transport occurs between 20 and 50 cm at these sites as well. The samples from the lower heights at these sites were physically observed to contain aggregated fine particles. These aggregated particles might aerodynamically act as larger particles, and thus be too coarse to suspend without some means to disaggregate them.

The two mesquite sites (M-NORT and M-RABB) and the artificially devegetated site (SCRAPE) had nearly identical PSDs at 5, 10, and 20 cm heights, with the sediment at 50 cm only slightly finer than lower heights (a decrease in median particle size of less than 50 μm from 20 to 50 cm), and the 100 cm height strongly shifted to finer particles (a decrease of over 100 μm from 50 to 100 cm) (Fig. 2). For these sites, the transition from saltation-dominated to suspension-dominated likely occurs between 50 and 100 cm.

Most sites had generally similar PSDs at each of the BSNE towers, as seen in the small standard deviation error bars in Fig. 2. However, at T-WEST and P-TOBO, the two sites with the greatest percentages of fine particles, there was greater variation between the PSDs for each tower. For example, at T-WEST towers 1 and 3 had more than 60% dust-sized particles collected at 5 cm above the surface, while the other two towers had less than 30% dust-sized particles at 5 cm.

3.1.2. Comparisons of PSDs between sites at each height

Comparisons of the median particle size at each height independently showed significant differences between the sites (ANOVA, $p < 0.0001$ for all heights, Table 2) (Figs. 3 and 4). Comparisons of the sites using the Tukey–Kramer post hoc test showed that certain sites tended to cluster together at all heights (Table 3A). At the coarser sizes, M-NORT and SCRAPE always had median particle sizes that were statistically identical, while at the finer sizes P-TOBO and T-WEST were statistically identical. The other sites grouped in different ways as the sample height changed, tending to be more similar to the coarser M-NORT and SCRAPE sites at lower heights and then changing to be more similar to the finer P-TOBO and T-WEST sites at the upper heights, consistent with the transition to finer particles as height increased seen in the previous section (Figs. 3 and 4). At the 5 and 10 cm heights, all of the sites except for P-TOBO and T-WEST had statistically similar median particle sizes (Table 3A). The groupings begin to change at 20 cm, with some of the sites with coarser particles grouping with M-NORT and SCRAPE, while those with finer particles grouping with P-TOBO and T-WEST. At 50 cm, the median particle size at M-NORT and SCRAPE were significantly larger than all sites except one, a grassland site (G-IBPE). Finally, at 100 cm the differences in median particle size have lessened, with most of the sites being statistically indistinguishable. The PSDs generally became more similar above the transition from saltation to suspension, at 50 cm for most vegetated sites and at 100 cm for all sites (Figs. 3 and 4).

Table 2
Results from one-way ANOVA tests for median particle size, span, mass flux, and mass flux of particles smaller than 50 μm. Data were log-transformed as required for normality.

Height	Log transformed?	df	*F* ratio	*p*-Value
(A) Median particle size				
5 cm	N	11	11.8175	<0.0001
10 cm	N	11	14.7289	<0.0001
20 cm	N	11	21.8524	<0.0001
50 cm	Y	11	20.0596	<0.0001
100 cm	Y	11	7.6383	<0.0001
(B) Span				
5 cm	Y	11	7.835	<0.0001
10 cm	Y	11	13.5833	<0.0001
20 cm	Y	11	21.9683	<0.0001
50 cm	Y	11	9.7612	<0.0001
100 cm	Y	11	4.9422	<0.0001
(C) Mass flux				
5 cm	Y	11	20.8281	<0.0001
10 cm	Y	11	18.7698	<0.0001
20 cm	Y	11	25.6842	<0.0001
50 cm	Y	11	37.5941	<0.0001
100 cm	Y	11	45.3822	<0.0001
(D) Mass flux of dust-sized particles				
5 cm	Y	11	10.4237	<0.0001
10 cm	Y	11	7.2476	<0.0001
20 cm	Y	11	14.0001	<0.0001
50 cm	Y	11	38.1108	<0.0001
100 cm	Y	11	26.1116	<0.0001

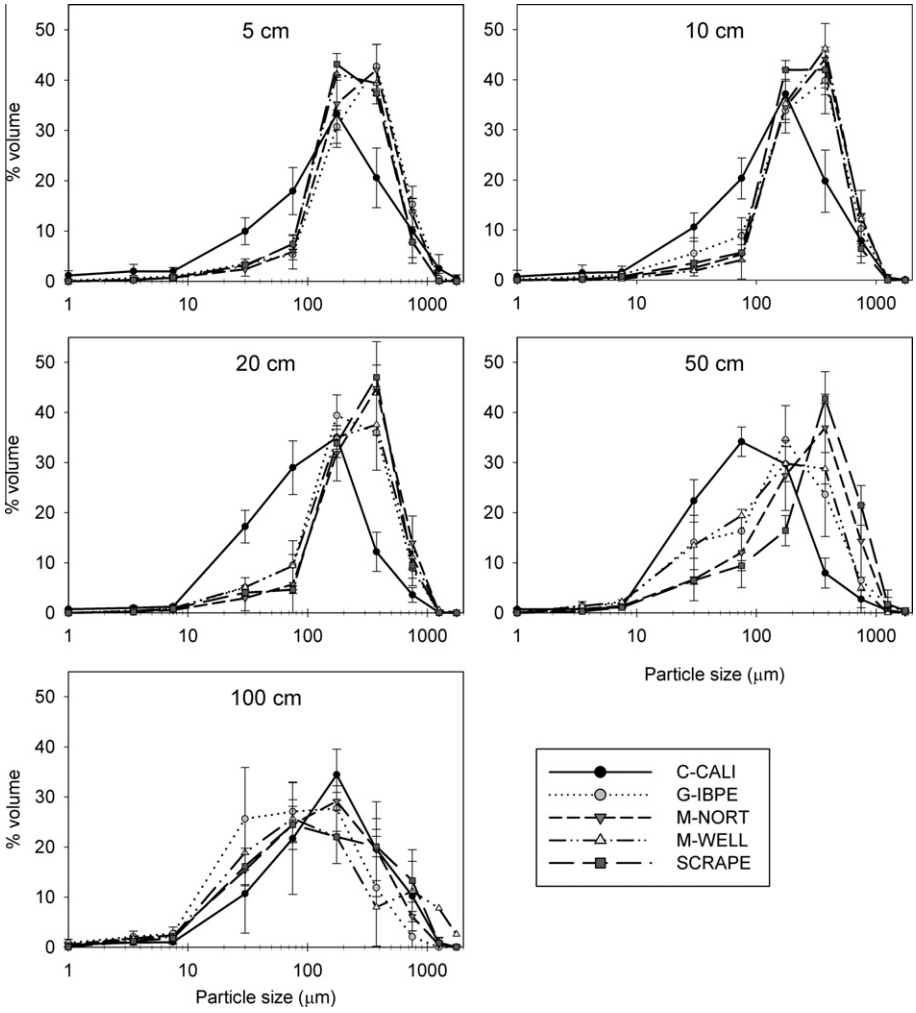

Fig. 3. Particle size distributions of representative sites with coarse particle sizes by height. At 5, 10, and 20 cm, the sites show two different patterns of PSDs. All of the sites except for C-CALI have very similar PSDs, while the PSD for C-CALI is shifted to finer particles. At 50 cm, C-CALI still have the PSD with the finest particles, G-IBPE and M-WELL have PSDs that have shifted to finer particles, and M-NORT and SCRAPE have similar and coarser PSDs. At 100 cm, the PSDs from all sites have largely converged, with median particle sizes of 80–120 μm.

Comparisons of the span of the PSDs (a measure of how peaked the PSD is, with small values indicating most of the particles are similar in size while larger values indicating a wider variation in sizes) at each height independently also showed significant differences between the sites (ANOVA, $p < 0.0001$ for all heights, Table 2). At 5, 10, and 20 cm, the Tukey–Kramer post hoc test indicated that sites P-TOBO and T-WEST grouped together with the largest spans, indicating the higher percentages of fine particles present at these sites (Table 3B). The two coarse sites, M-NORT and SCRAPE, also grouped together at all heights with narrow spans, indicating a fairly uniform population of particles (Table 3B). The remaining sites were generally intermediate to these different groups of sites. At lower heights they tended to group with the coarser sites because of their lack of fine particles, while at the upper heights they tended to group with the finer sites. Indeed, at 50 and 100 cm most of the sites were statistically indistinguishable.

3.2. Potential dust production

For all heights, there were significant differences in horizontal mass flux across the sites (ANOVA, $p < 0.0001$ for all sites, Table 2) (Fig. 5). The Tukey–Kramer post hoc test indicated that mass fluxes at M-NORT and SCRAPE were significantly greater than all other sites at 5, 20, 50, and 100 cm, and greater than all sites but T-TAYL at 10 cm (Table 4B). At 20, 50, and 100 cm, SCRAPE had significantly more mass flux than M-NORT. All other sites had statistically similar mass fluxes at all heights.

The percent of dust-sized particles ($\leqslant$50 μm) was greatest at the lower heights in the P-TOBO and T-WEST sites and least at the lower heights in the M-NORT and SCRAPE sites (Figs. 2 and 4). Multiplying the percent of dust-sized particles by the mass flux gave an estimate of dust production for all sites at all heights (Fig. 6). For all heights, there were significant differences in mass of dust-sized particles across all sites (ANOVA, $p < 0.0001$ for all heights, Table 2) (Fig. 6). Despite the differences in the *percent* of dust-sized particles, at 5 and 10 cm, the SCRAPE, M-NORT, P-TOBO, T-TAYL, and T-WEST sites were grouped together by the Tukey–Kramer post hoc test (Table 4B). For 20, 50, and 100 cm, SCRAPE had the greatest mass flux of dust-sized particles. At those same heights, M-NORT, P-TOBO, T-TAYL, T-WEST, and G-BASN had greater mass flux of dust-sized particles than the other sites (Table 4B and Fig. 6).

4. Discussion

4.1. Aeolian particle size distributions in the Jornada Basin

The particle size distributions for most sites were similar, with most of the samples from 5, 10, and 20 cm made up largely by

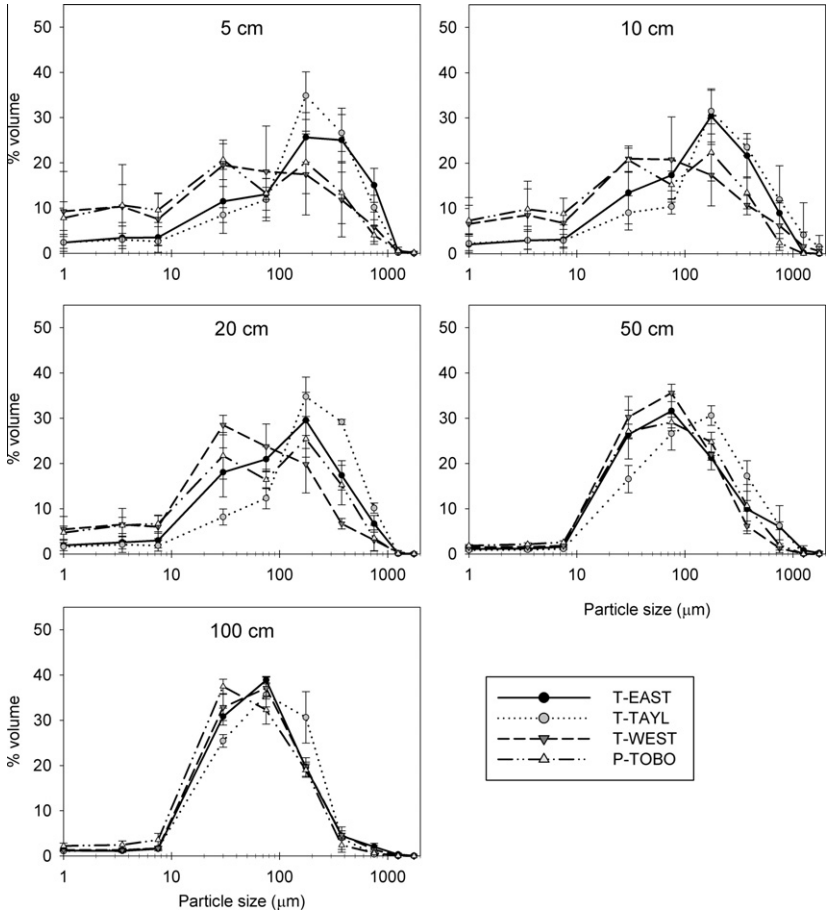

Fig. 4. Particle size distributions of representative sites with fine particle sizes by height. At 5 and 10 cm, T-WEST and P-TOBO have similar PSDs with a higher percentage of finer particles, while T-EAST and T-TAYL have similar and coarser PSDs. At 50 and 100 cm, the PSDs from all sites have largely converged, with median particle sizes of 50–70 μm.

Table 3
Results from the Tukey–Kramer post hoc means comparison for (A) median particle size and (B) span. The averages reported in the table have been back-transformed if the values had been log-transformed for the ANOVA. Samples with means that cannot be distinguished statistically are joined with the same letter. The sites are reported in the same order for both tables. The results for sites P-TOBO and T-WEST are bolded because they always are grouped together. The results for sites M-NORT and SCRAPE are italicized because they always are grouped together. The other sites are generally intermediate to these two groups. The particle size distributions tend to become more similar as the height above the soil surface increases.

	5 cm Mean				10 cm Mean						20 cm Mean						50 cm Mean						100 cm Mean			
(A) Median particle size																										
C-CALI	175.6	A			159.5	A					133.2		B	C	D		96.5			C	D	E	F	78.7		B	C
C-GRAV	175.3	A			125.9	A	B				141.0		B	C			119.3			C	D	E		76.7		B	C
C-SAND	228.6	A			157.2	A					143.7		B	C			98.2			C	D	E	F	80.1	A	B	C
G-BASN	380.7	A			263.0	A					181.4	A	B	C			112.3			C	D	E	F	73.4		B	C
G-IBPE	286.3	A			246.8	A					226.4	A	B				164.7		B	C				84.1	A	B	C
G-SUMM	233.0	A			205.5	A					143.3		B	C			133.5			C	D			75.7		B	C
T-EAST	168.7	A			135.5	A	B				109.7			C	D		77.2				D	E	F	64.5			C
T-TAYL	185.7	A			206.5	A					197.4	A	B	C			111.5			C	D	E	F	74.6		B	C
T-WEST	**37.7**		**B**		**49.2**		**B**				**53.3**					**E**	**66.0**						**F**	**62.5**			**C**
P-TOBO	**46.9**		**B**		**50.3**		**B**				**79.5**				**D**	**E**	**73.1**					**E**	**F**	**54.1**			**C**
M-NORT	*270.8*	*A*			*274.1*	*A*					*277.7*	*A*					*245.8*	*A*	*B*					*119.6*	*A*		
SCRAPE	*232.8*	*A*			*243.6*	*A*					*273.1*	*A*					*336.8*	*A*						*123.8*	*A*	*B*	
(B) Span																											
C-CALI	3.40	A	B	C	2.59			C	D	E	2.77		B	C			2.79		B	C				2.63		B	C
C-GRAV	2.97		B	C	3.28		B	C			2.55			C	D		3.06	A	B					2.65		B	C
C-SAND	2.56			C	3.10		B	C	D		2.94		B	C			4.60	A						2.64		B	C
G-BASN	2.00			C	2.41			C	D	E	2.82		B	C	D		3.82	A	B					3.05	A	B	C
G-IBPE	1.68			C	1.72			C	D	E	1.76				D	E	F	2.50		B	C				2.90	A	B	C
G-SUMM	2.41			C	2.36			C	D	E	3.56	A	B	C				3.10	A	B					2.32		B	C
T-EAST	3.29	A	B	C	3.30		B	C	D		3.66	A	B	C				4.21	A	B					2.47		B	C
T-TAYL	2.57		B	C	2.98		B	C	D		2.37			C	D	E		3.43	A	B					2.25			C
T-WEST	**9.15**	**A**			**8.27**	**A**					**4.85**	**A**						**2.74**		**B**	**C**				**2.48**		**B**	**C**
P-TOBO	**7.35**	**A**	**B**		**6.18**	**A**	**B**				**4.24**	**A**	**B**					**3.64**	**A**	**B**					**2.72**		**B**	**C**
M-NORT	*1.56*			*C*	*1.47*					*E*	*1.47*						*F*	*1.91*			*C*				*3.30*	*A*	*B*	
SCRAPE	*1.62*			*C*	*1.45*				*D*	*E*	*1.43*					*E*	*F*	*1.76*			*C*				*4.35*	*A*		

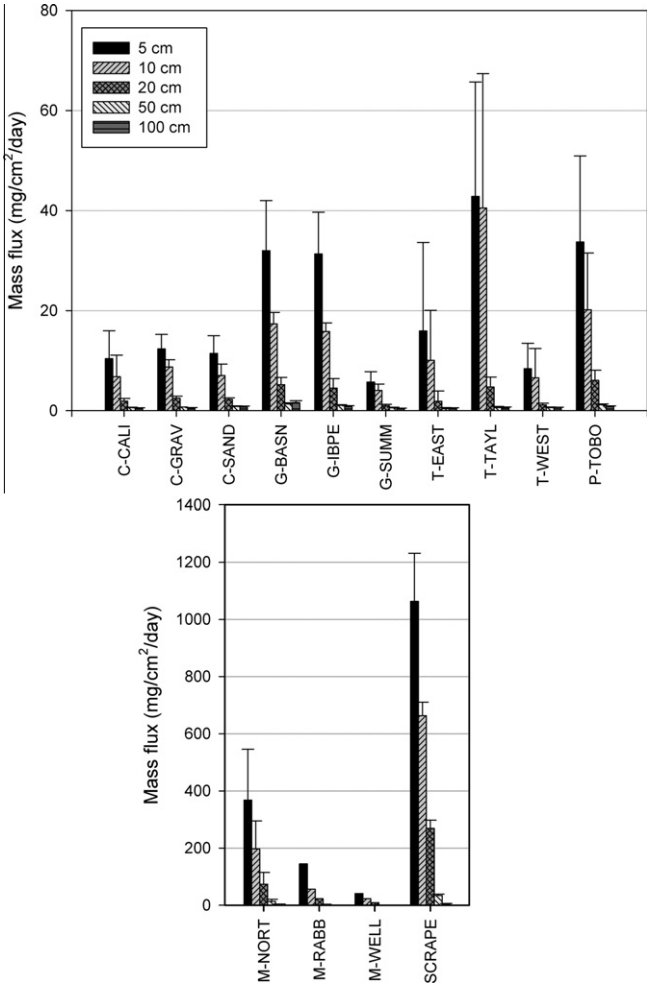

Fig. 5. Sediment horizontal mass flux by height for all sites. For all sites, the horizontal mass flux is greatest at the lower heights and decreases with increasing height above the soil surface. Mass flux is dominated by the artificially-devegetated SCRAPE site, while M-NORT dominates the vegetated sites. The three mesquite sites differ in the development of large dunes, with M-NORT having the most developed dunes and the largest inter-shrub distances. M-WELL has the least developed dunes and the most vegetative cover of the mesquite sites, and also has the least mass flux of the mesquite sites. However, M-WELL still has slightly greater mass flux than the other vegetated sites. Of those sites, P-TOBO, T-TAYL, G-BASN, and G-IBPE has the greatest mass flux.

sand-sized particles, being within the saltation zone (Figs. 2–4). Only P-TOBO and T-WEST, the sites that were grouped together for median particle size and span by the Tukey–Kramer test at those lower heights, had large percentages of clay- and silt-sized particles near the ground. Soil classification of all study sites by the National Soil Survey Lab (Soil Survey Staff, 2009) shows that most sites range from sandy loams to loams (Table 1). The only exceptions included in this study are two tarbush sites (T-WEST and T-TAYL), classified as sandy clay loams, and the playa site (P-TOBO), classified as a clay loam (Soil Survey Staff, 2009). Laboratory tests have shown that the median particle size of aeolian emissions from soils decreases as soil clay content increases (Carvacho et al., 2001; Zobeck and Amante-Orozco, 2001), as we observed in this study. This pair of sites also showed the greatest variation between PSDs from samples collected in the field at different towers within the same site: at T-WEST towers 1 and 3 had more than 60% dust-sized particles collected at 5 cm above the surface, while the other two towers had less than 30% dust-sized particles at 5 cm. Laboratory dust emission tests (Ashbaugh et al., 2003; Zobeck and Amante-Orozco, 2001) have shown significant variations in dust emissions within the same soil at the same site, especially for clayey wind-erodible soils (Zobeck and Amante-Orozco, 2001). Studies of individual dust events in southwest North America (Gillette, 1999; Lee et al., 2009) have similarly pointed out strong spatial heterogeneities in aerosol emission, with contiguous, identical-appearing "patches" of playas and shrublands alternately emitting or stable at the same moment during a storm. The observed variations of PSD at different towers within a given site may also be a manifestation of this small-scale variability in wind erosion.

The transition from saltation-dominated transport to suspension-dominated transport (Fryrear and Saleh, 1993) occurred around 20 cm for most sites. For all sites except P-TOBO and T-WEST, the shift was from coarser particles to finer particles, as would be expected *a priori*. For P-TOBO and T-WEST, two of the dust-emitting sites with relatively clayey surfaces, the finer particles apparently agglomerated as a surface crust and were likely transported as larger-sized, flattened aggregates typical of wind-eroded clayey surface crusts (Cahill et al., 1996), remaining less than 20 cm from the soil surface. During the particle size analysis, these agglomerates were largely disaggregated through physical processes, allowing individual particle sizes to be measured. Without additional forces, such as saltating particles "sand-blasting" the surface (Gillette and Chen, 1999) to cause this disaggregation *in situ*, we could overestimate the dust production from these sites (Chandler et al., 2005). However, a disproportionate amount of dust emission in the CD has been observed at geomorphic interfaces where sandblasting would occur, such as playa–sand sheet contacts (Lee et al., 2009; Rivera Rivera et al., 2010), thus the laboratory analysis may have simulated actual geomorphic processes to some extent.

For M-NORT, M-RABB, and SCRAPE, the sites with the largest overall aeolian mass fluxes (and with PSDs statistically grouped together), the transition height from saltation to suspension was higher than at the other sites, occurring closer to 50 cm above the soil surface. The lack of vegetation to protect the soil surface likely caused the wind energy to be greater than in sites with more vegetation, leading to an increased intensity of saltation at those sites and lifting more of the larger sand-sized particles higher above the surface (Chen et al., 1996; Dong et al., 2003).

4.2. Aeolian mass fluxes and dust fluxes in the Jornada Basin

The horizontal mass fluxes during the period sampled for this study, spring 2006, followed the same patterns found by Gillette and Chen (2001), Gillette and Pitchford (2004), and Bergametti and Gillette (2010). The artificially devegetated site SCRAPE had a statistically significant highest horizontal mass flux of all sites (Fig. 5), which is expected since removal of vegetation and surface crusts increases the erodibility of sandy desert soils (J. Li et al., 2007; X.Y. Li 2004), and in line with observations of disturbed lands in the CD as "hotspots" of dust emission (Gill et al., 2009; Lee et al., 2009; Rivera Rivera et al., 2010). This is also in agreement with prior studies of the SCRAPE site (Gillette and Chen, 2001).

Of the vegetated sites, M-NORT had significantly greater horizontal mass flux than the other sites, and M-RABB had the next greatest amount. The remaining sites had low and relatively similar amounts of mass flux (Fig. 5). M-NORT has the most developed "streets" (long, unvegetated, wind-parallel stretches) of the three mesquite sites (Gillette et al., 2006; Gillette and Pitchford, 2004; Okin and Gillette, 2001): such long fetches would result in increased aeolian flux with distance through the "Owen Effect" in an area already meeting the requirements of an aeolian "hot spot" (Gillette, 1999). On the other hand, M-WELL, the mesquite site with little development of streets, had similar mass fluxes to some

Table 4
Results from the Tukey–Kramer post hoc means comparison for (A) mass flux and (B) mass flux of particles smaller than 50 μm. All of the averages reported in the table have been back-transformed from the log-transformation required for the ANOVA. Samples with means that cannot be distinguished statistically are joined with the same letter. The sites are reported in the same order for both tables. The results for sites P-TOBO and T-WEST are bolded because they always are grouped together. The results for sites M-NORT and SCRAPE are italicized because they tend to group together. The other sites are generally intermediate to these two groups.

	5 cm Mean						10 cm Mean						20 cm Mean						50 cm Mean						100 cm Mean					
(A) Mass flux																														
C-CALI	9.51		B				6.00			C	D		1.84			C	D		0.596			C			0.441				D		
C-GRAV	12.1		B				8.65			C	D		2.44			C	D		0.723			C			0.570				D		
C-SAND	11.1		B				6.80			C	D		2.24			C	D		0.839			C			0.705				D		
G-BASN	30.9		B				17.2			C	D		5.07			C	D		1.32			C			1.57			C			
G-IBPE	30.3		B				15.7			C	D		4.23			C	D		1.05			C			0.764				D		
G-SUMM	5.45		B				3.90				D		0.967				D		0.564			C			0.482				D		
T-EAST	9.46		B				7.27			C	D		0.995			C	D		0.359			C			0.452				D		
T-TAYL	37.2		B				31.0		B	C			4.36			C	D		0.613			C			0.627				D		
T-WEST	**7.46**		**B**				**5.08**			**C**	**D**		**1.12**			**C**	**D**		**0.604**			**C**			**0.638**				**D**		
P-TOBO	**29.8**		**B**				**17.8**			**C**	**D**		**5.76**			**C**			**1.20**			**C**			**0.796**			**C**	**D**		
M-NORT	*269.1*	*A*					*146.6*	*A*	*B*				*53.6*		*B*				*10.4*		*B*				*2.84*		*B*				
SCRAPE	*1054.4*	*A*					*661.8*	*A*					*267.6*	*A*					*33.9*	*A*					*5.42*	*A*					
(B) Mass flux of particles smaller than 50 μm																														
C-CALI	1.20				D	E	0.740			C	D		0.284			C			0.122				D	E	0.117						F
C-GRAV	1.31				D	E	1.38		B	C	D		0.312			C			0.108				D	E	0.158					E	F
C-SAND	0.706					E	0.726			C	D		0.257			C			0.166				D	E	0.171					E	F
G-BASN	1.38			C	D	E	0.942		B	C	D		0.564		B	C			0.248			C	D		0.453		B	C			
G-IBPE	1.49				D	E	1.03		B	C	D		0.258			C			0.170				D	E	0.222				D	E	
G-SUMM	0.555					E	0.392				D		0.178			C			0.092					E	0.133					E	F
T-EAST	1.46			C	D	E	1.28		B	C	D		0.240			C			0.107				D	E	0.157					E	F
T-TAYL	6.01	A	B	C	D		4.61	A	B	C			0.550		B	C			0.118				D	E	0.184				D	E	F
T-WEST	**3.10**		**B**	**C**	**D**	**E**	**2.02**		**B**	**C**	**D**		**0.510**		**B**	**C**			**0.210**			**C**	**D**		**0.236**			**C**	**D**	**E**	
P-TOBO	**13.70**	**A**	**B**				**8.02**	**A**	**B**				**2.21**		**B**				**0.402**			**C**			**0.362**		**B**	**C**	**D**		
M-NORT	*8.05*	*A*	*B*	*C*			*4.19*	*A*	*B*	*C*			*1.57*		*B*				*0.813*		*B*				*0.559*		*B*				
SCRAPE	*43.32*	*A*					*27.71*	*A*					*13.28*	*A*					*2.64*	*A*					*1.02*	*A*					

of the other vegetated sites, such as G-IBPE and P-TOBO (Fig. 5). This shows that even within sites dominated by the same types of vegetation, the specific orientation of the vegetation and bare soil areas relative to the prevailing wind direction influences aeolian emission flux; thus, knowledge of vegetation type alone may be insufficient to predict aeolian emissions in some environments. Horizontal mass flux at the devegetated site was approximately triple that of the mesquite site with the largest intershrub distances (although the particle size distributions of the material were similar at both sites). This suggests that although the transported particles have similar size distributions, the mesquite dunes at the Jornada LTER provide some protection from wind erosion, albeit less than other vegetation types provide (Li et al., 2007).

The devegetated site and M-NORT (the site with well-developed mesquite streets) had the lowest *percentages* of dust-sized particles, as a fraction of total aeolian material, of all the sites. However, the devegetated site had the greatest *mass flux* of dust-sized particles at all heights, and M-NORT was among the sites with the highest dust *mass flux* of all vegetated sites (Fig. 6), due to the much greater total aeolian mass flux from these sites. The playa site (P-TOBO) had aeolian dust mass flux similar to M-NORT, while the tarbush sites had lower fluxes than P-TOBO and M-NORT, but still higher dust fluxes than the other sites (Fig. 6). These sites demonstrate two different mechanisms of dust production in the Chihuahuan Desert. The playa site is a relatively major dust producer due to its high overall proportion of fine particles, whereas M-NORT (and the devegetated site as well) is a major dust producer because of its far greater overall aeolian mass flux. The tarbush site T-WEST had the greatest overall proportion of dust particles emitted, but lower horizontal aeolian mass flux than the playa site, thus decreasing its rank in the system. Tarbush sites T-TAYL and T-EAST represent an intermediate condition, with lower percentages of dust-sized particles but greater mass fluxes than T-WEST, giving the tarbush sites similar amounts of dust-sized mass flux. Accounting for the differential mass flux of aeolian particles produced by each vegetation type, the total mass of dust per unit area produced by each vegetation type at the Jornada Basin LTER is greatest at the anthropogenically-disturbed SCRAPE site, the P-TOBO playa site, the M-NORT mesquite site with "streets," and the tarbush sites, while creosote bush, grassland, and the other two mesquite sites produce the least dust.

4.3. Effects of land cover on dust emission in the Jornada Basin

Playas have long been noted as sources for dust emission (Gill, 1996; Prospero et al., 2002; Engelstaedter et al., 2003; Bullard et al., 2008), and in the CD, playas and anthropogenically-disturbed lands are the predominant overall initiation points of dust "plumes" visible on satellite images (Gill et al., 2009; Rivera Rivera et al., 2010). Playa surfaces will have low threshold friction velocities and aerodynamic roughness lengths, increasing their wind erodibility (Gillette, 1999). Playa edges often comprise contact areas between saltating sandy sediments and finer lacustrine sediments (Bullard et al., 2008), providing ideal foci and initiation sites for dust production via saltation/sandblasting (Gillette and Chen, 2001; Rivera Rivera et al., 2010). However, during the most intense and regionally widespread dust storms, when wind strengths would be sufficient to initiate erosion across multiple land surface types and penetrate unvegetated gaps in shrublands (Okin et al., 2006), almost as many (Lee et al., 2009) or the majority of (Rivera Rivera et al., 2010) dust plumes in the region emanate from shrublands (which would include the wind-aligned "streets") as from playas.

The results of those remote-sensing-based studies and this field-based monitoring at Jornada illustrate how different landforms and land cover classes can contribute in different ways to regional dust loading. While playas and anthropogenically-disturbed lands in the northern CD are the most easily eroded and most intense producers of dust per unit land area, shrublands, especially those dominated by mesquite and tarbush, may produce more dust

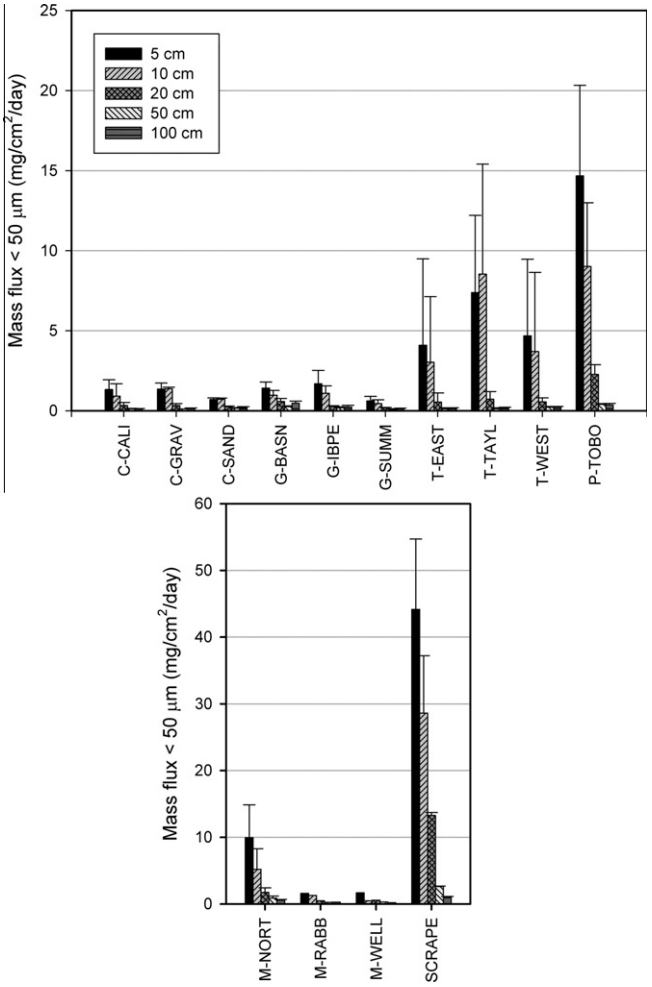

Fig. 6. Percent of dust-sized (⩽50 μm) sediment horizontal mass flux by height for all sites. The devegetated SCRAPE site had the greatest amount of dust-sized mass flux, about 3× more than the next largest producer, P-TOBO. M-NORT and the three tarbush sites produced less dust-sized mass flux than P-TOBO, but more than the other vegetated sites.

overall due to their larger spatial coverage coupled with their potential for high total aeolian mass flux. Within the Jornada Basin itself, since mesquite presently covers ~60% of the land area (Gibbens et al., 2005), mesquite-dominated shrublands have the potential to produce the most dust, while playas and tarbush-dominated alluvial flats (which cover about 8%) have the potential to produce large amounts of dust if the conditions are correct. This is in line with the suggestions of Reheis and Kihl (1995), who suggested that alluvial sources ultimately produce a greater volume of dust than playas in the southwest Great Basin and Mojave Desert due to their greater areal extent. Continued expansion of mesquite in the Jornada Basin (and elsewhere in the Chihuahuan Desert) would therefore be expected to lead to increased dust production.

5. Summary and Conclusions

Analysis of aeolian samples collected in the field in different vegetation communities of the Jornada Basin has shed light on the impacts of land cover on dust emission and potential changes in intensity of aeolian processes with vegetation change. Aeolian mass fluxes measured in the field in the Jornada Basin are in broad agreement with remote-sensing-based analyses of dust events across the Chihuahuan Desert, indicating that playas and bare soil areas (whether formed through anthropogenic disturbance or the natural development of "mesquite streets") provide the least resistance to aeolian erosion and are the focal points of dust emission in the region, although the contribution of shrublands cannot be ignored due to their spatial extent and potential for high overall aeolian mass flux. Differing aeolian fluxes within different mesquite dune sites illustrate that within certain vegetation communities, the specific orientation of vegetation and bare soil areas relative to the prevailing wind direction influences aeolian emission flux.

The total mass of dust emitted per unit area in the Jornada Basin is greatest at the anthropogenically-disturbed SCRAPE site, the P-TOBO playa site, the M-NORT mesquite site with "streets," and the tarbush sites, while creosote bush, grassland, and the other two mesquite sites produce lesser amounts of dust. The vegetation communities of the Jornada Basin illustrate two different mechanisms of dust production in drylands. At some sites, such as playas, dust production is driven by high overall proportion of fine particles emitted, while at other sites, such as mesquite dunes with "streets," dust production is driven by high overall aeolian mass flux. As mesquite shrublands continue to expand in the Jornada Basin at the expense of grasslands, dust production and total aeolian sediment flux should increase.

This study has also suggested that effects of soil texture on dust particle size, the intrasite variation of dust particle size, and the increasing height of transition from saltation to suspension with increasing mass flux and saltation intensity, as derived from laboratory studies, are confirmed in the field.

Acknowledgements

This project was supported in part by NOAA through the Educational Partnership Program for Minority Serving Institutions (EPP/MSI) Cooperative Agreement NA17AE1623, and by the Texas Higher Education Coordinating Board through Norman Hackerman Advanced Research Projects Grant 003661-0027-2007. The authors thank Dale Gillette for collecting the samples and providing them for analysis.

Appendix A. Supplementary data

Supplementary data associated with this article can be found, in the online version, at doi:10.1016/j.aeolia.2011.02.002.

References

Altesor, A., Pineiro, G., Lezama, F., Jackson, R.B., Sarasola, M., Paruelo, J.M., 2006. Ecosystem changes associated with grazing in subhumid South American grasslands. J. Veg. Sci. 17, 323–332.

Angassa, A., 2005. The ecological impact of bush encroachment on the yield of grasses in Borana rangeland ecosystem. Afr. J. Ecol. 43, 14–20.

Archer, S., Scifres, C., Bassham, C.R., Maggio, R., 1988. Autogenic succession in a subtropical savanna – conversion of grassland to thorn woodland. Ecol. Monogr. 58, 111–127.

Ashbaugh, L.L., Carvacho, O.F., Brown, M.S., Chow, J.C., Watson, J.G., Magliano, K.C., 2003. Soil sample collection and analysis for the fugitive dust characterization study. Atmos. Environ. 37, 1163–1173.

Belnap, J., Gillette, D.A., 1998. Vulnerability of desert biological soil crusts to wind erosion: the influences of crust development, soil texture, and disturbance. J. Arid Environ. 39, 133–142.

Beltrán-Przekurat, A., Pielke, R.A., Peters, D.P.C., Snyder, K.A., Rango, A., 2008. Modeling the effects of historical vegetation change on near-surface atmosphere in the northern Chihuahuan Desert. J. Arid Environ. 72, 1897–1910.

Bergametti, G., Gillette, D.A., 2010. Aeolian sediment fluxes measured over various plant/soil complexes in the Chihuahuan desert. J. Geophys. Res. 115, F03044. doi:10.1029/2009jf001543.

Bowker, G.E., Gillette, D.A., Bergametti, G., Marticorena, B., 2006. Modeling flow patterns in a small vegetated area in the northern Chihuahuan Desert using QUIC (Quick Urban & Industrial Complex). Environ. Fluid Mech. 6, 359–384.

Bowker, G.E., Gillette, D.A., Bergametti, G., Marticorena, B., Heist, D.K., 2008. Fine-scale simulations of aeolian sediment dispersion in a small area in the northern Chihuahuan Desert. J. Geophys. Res. 113, F02S11. doi:10.1029/2007JF000748.

Bullard, J., Baddock, M., McTainsh, G., Leys, J., 2008. Sub-basin scale dust source geomorphology detected using MODIS. Geophys. Res. Lett. 35, L15404. doi:10.1029/2008GL033928.

Cabral, A.C., De Miguel, J.M., Rescia, A.J., Schmitz, M.F., Pineda, F.D., 2003. Shrub encroachment in Argentinean savannas. J. Veg. Sci. 14, 145–152.

Cahill, T.A., Gill, T.E., Reid, J.S., Gearhart, E.A., Gillette, D.A., 1996. Saltating particles, playa crusts and dust aerosols at Owens (dry) Lake, California. Earth Surf. Proc. Land. 21, 621–639.

Carvacho, O.F., Ashbaugh, L.L., Brown, M.S., Flocchini, R.G., 2001. Relationship between San Joaquin Valley soil texture and PM_{10} emission potential using the UC Davis dust resuspension test chamber. Trans. ASAE 44, 1603–1608.

Chandler, D.G., Saxton, K.E., Busacca, A.J., 2005. Predicting wind erodibility of loessial soils in the Pacific Northwest by particle sizing. Arid Land Res. Manag. 19, 13–27.

Chen, W.N., Yang, Z.T., Zhang, J.S., Han, Z.W., 1996. Vertical distribution of wind-blown sand flux in the surface layer, Taklamakan Desert, Central Asia. Phys. Geogr. 17, 193–218.

Cheng, X.L., An, S.Q., Liu, S.R., Li, G.Q., 2004. Micro-scale spatial heterogeneity and the loss of carbon, nitrogen and phosphorus in degraded grassland in Ordos Plateau, northwestern China. Plant Soil 259, 29–37.

Costello, D.A., Lunt, I.D., Williams, J.E., 2000. Effects of invasion by the indigenous shrub Acacia sophorae on plant composition of coastal grasslands in south-eastern Australia. Biol. Conserv. 96, 113–121.

Dominguez Acosta, M., 2009. The Pluvial Lake Palomas-Samalayuca Dunes System. Ph.D. dissertation, (Geology), University of Texas at El Paso.

Dong, Z., Liu, X., Wang, H., Zhao, A., Wang, X., 2003. The flux profile of a blowing sand cloud: a wind tunnel investigation. Geomorphology 49, 219–230.

Engelstaedter, S., Kohfeld, K.E., Tegen, I., Harrison, S.P., 2003. Controls of dust emissions by vegetation and topographic depressions: an evaluation using dust storm frequency data. Geophys. Res. Lett. 30, 6. doi:10.1029/2002gl016471.

Fryrear, D.W., 1986. A field dust sampler. J. Soil Water Conserv. 41, 117–120.

Fryrear, D.W., Saleh, A., 1993. Field wind erosion – vertical distribution. Soil Sci. 155, 294–300.

Gibbens, R.P., McNeely, R.P., Havstad, K.M., Beck, R.F., Nolen, B., 2005. Vegetation changes in the Jornada Basin from 1858 to 1998. J. Arid Environ. 61, 651–668.

Gill, T., Mbuh, M., Dominguez, M., Lee, J., Baddock, M., Lee, C., Whitehead, S., Rivera Rivera, N., Peinado, P., 2009. Geomorphology of MODIS-visible dust plumes in the Chihuahuan Desert-preliminary results. EOS Trans. AGU 90, EP21A-0569.

Gill, T.E., 1996. Eolian sediments generated by anthropogenic disturbance of playas: human impacts on the geomorphic system and geomorphic impacts on the human system. Geomorphology 17, 207–228.

Gillette, D.A., 1999. A qualitative geophysical explanation for "Hot Spot" dust emitting source regions. Contr. Atmos. Phys. 72, 67–77.

Gillette, D.A., Chen, W., 1999. Size distributions of saltating grains: an important variable in the production of suspended particles. Earth Surf. Proc. Land. 24, 449–462.

Gillette, D.A., Chen, W.A., 2001. Particle production and aeolian transport from a "supply-limited" source area in the Chihuahuan desert, New Mexico, United States. J. Geophys. Res. 106 (D6), 5267–5278.

Gillette, D., Monger, H.C., 2006. Eolian processes on the Jornada Basin. In: Havstad, K.M., Huenneke, L.F., Schlesinger, W.H. (Eds.), Structure and function of a Chihuahuan Desert ecosystem: the Jornada Basin long-term ecological research site. Oxford University Press, Oxford, New York, pp. 189–210.

Gillette, D.A., Pitchford, A.M., 2004. Sand flux in the northern Chihuahuan desert, New Mexico, USA, and the influence of mesquite-dominated landscapes. J. Geophys. Res. 109, F04003. doi:10.1029/2003JF000031.

Gillette, D.A., Herrick, J.E., Herbert, G.A., 2006. Wind characteristics of mesquite streets in the northern Chihuahuan Desert, New Mexico, USA. Environ. Fluid Mech. 6, 241–275.

Ginoux, P., Chin, M., Tegen, I., Prospero, J.M., Holben, B., Dubovik, O., Lin, S.J., 2001. Sources and distributions of dust aerosols simulated with the GOCART model. J. Geophys. Res. 106 (D17), 20255–20273.

Ginoux, P., Prospero, J.M., Torres, O., Chin, M., 2004. Long-term simulation of global dust distribution with the GOCART model: correlation with North Atlantic Oscillation. Environ. Model. Softw. 19, 113–128.

Goossens, D., Offer, Z.Y., 2000. Wind tunnel and field calibration of six aeolian dust samplers. Atmos. Environ. 34, 1043–1057.

Hesse, P.P., Simpson, R.L., 2006. Variable vegetation cover and episodic sand movement on longitudinal desert sand dunes. Geomorphology 81, 276–291.

Huenneke, L.F., Anderson, J.P., Remmenga, M., Schlesinger, W.H., 2002. Desertification alters patterns of aboveground net primary production in Chihuahuan ecosystems. Glob. Change Biol. 8, 247–264.

Huenneke, L.F., Clason, D., Muldavin, E., 2001. Spatial heterogeneity in Chihuahuan Desert vegetation: implications for sampling methods in semi-arid ecosystems. J. Arid Environ. 47, 257–270.

Kraaij, T., Milton, S.J., 2006. Vegetation changes (1995–2004) in semi-arid Karoo shrubland, South Africa: effects of rainfall, wild herbivores and change in land use. J. Arid Environ. 64, 174–192.

Lee, J.A., Gill, T.E., Mulligan, K.R., Acosta, M.D., Perez, A.E., 2009. Land use/land cover and point sources of the 15 December 2003 dust storm in southwestern North America. Geomorphology 105, 18–27.

Li, J., Okin, G., Alvarez, L., Epstein, H., 2007. Quantitative effects of vegetation cover on wind erosion and soil nutrient loss in a desert grassland of southern New Mexico, USA. Biogeochemistry 85, 317–332.

Li, X.Y., Liu, L.Y., Wang, J.H., 2004. Wind tunnel simulation of aeolian sandy soil erodibility under human disturbance. Geomorphology 59, 3–11.

Mahowald, N.M., Zender, C.S., Luo, C., Savoie, D., Torres, O., del Corral, J., 2002. Understanding the 30-year Barbados desert dust record. J. Geophys. Res. 107, D21. doi:10.1029/2002JD002097.

Okin, G., Parsons, A., Wainwright, J., Herrick, J., Bestelmeyer, B., Peters, D., Fredrickson, E., 2009. Do changes in connectivity explain desertification? Bioscience 59, 237–244.

Okin, G.S., Gillette, D.A., 2001. Distribution of vegetation in wind-dominated landscapes: implications for wind erosion modeling and landscape processes. J. Geophys. Res. 106 (D9), 9673–9683.

Okin, G.S., Gillette, D.A., Herrick, J.E., 2006. Multi-scale controls on and consequences of aeolian processes in landscape change in arid and semi-arid environments. J. Arid Environ. 65, 253–275.

Peters, D.P.C., Bestelmeyer, B.T., Herrick, J.E., Fredrickson, E.L., Monger, H.C., Havstad, K.M., 2006. Disentangling complex landscapes: new insights into arid and semiarid system dynamics. Bioscience 56, 491–501.

Peters, D.P.C., Gibbens, R.P., 2006. Plant communities in the Jornada Basin: the dynamic landscape. In: Havstad, K.M., Huenneke, L.F., Schlesinger, W.H. (Eds.), Structure and Function of a Chihuahuan Desert Ecosystem: The Jornada Basin Long-term Ecological Research Site. Oxford University Press, Oxford, New York, pp. 211–231.

Prospero, J.M., Ginoux, P., Torres, O., Nicholson, S.E., Gill, T.E., 2002. Environmental characterization of global sources of atmospheric soil dust identified with the Nimbus 7 Total Ozone Mapping Spectrometer (TOMS) absorbing aerosol product. Rev. Geophys. 40 (1), 1022. doi:10.1029/2000RG000095.

Reheis, M.C., Kihl, R., 1995. Dust deposition in southern Nevada and California, 1984–1989: relations to climate, source area, and source lithology. J. Geophys. Res. 100 (D5), 8893–8918.

Reynolds, R., Reheis, M., Hinkley, T., Tigges, R., Clow, G., Lamothe, P., Yount, J., Meeker, G., Chavez, P., Mackinnon, D., Velasco, M., Sides, S., Soltesz, D., Lancaster, N., Miller, M., Fulton, R., Belnap, J., 2003. Dust emission and deposition in the Southwestern United States – integrated field, remote sensing, and modeling studies to evaluate response to climatic variability and land use. In: Alsharhan, A.S., Wood, W.W., Goudie, A.S., Fowler, A., Abdellatif, E.M. (Eds.), Desertification in the Third Millennium. Swets and Seitlinger, Lisse, The Netherlands, pp. 271–282.

Reynolds, R.L., Yount, J.C., Reheis, M., Goldstein, H., Chavez, P., Fulton, R., Whitney, J., Fuller, C., Forester, R.M., 2007. Dust emission from wet and dry playas in the Mojave desert, USA. Earth Surf. Process. Land. 32, 1811–1827.

Rivera Rivera, N.I., Gill, T.E., Bleiweiss, M.P., Hand, J.L., 2010. Source characteristics of hazardous Chihuahuan Desert dust outbreaks. Atmos. Environ. 44, 2457–2468.

Safriel, U., Adeel, Z., 2005. Dryland systems. In: Hassan, R., Scholes, R., Ash, N. (Eds.), Ecosystems and Human Well-being: Current State and Trends, Findings of the Condition and Trends Working Group. Island Press, Washington, DC, pp. 623–662.

Scholes, R.J., Archer, S.R., 1997. Tree–grass interactions in savannas. Annu. Rev. Ecol. Syst. 28, 517–544.

Shao, Y., McTainsh, G.H., Leys, J.F., Raupach, M.R., 1993. Efficiencies of sediment samplers for wind erosion measurement. Aust. J. Soil Res. 31, 519–532.

Soil Survey Staff, 2009. National Soil Survey Characterization Data. Soil Survey Laboratory, National Soil Survey Center, USDA-NRCS, Lincoln, NE.

Sperazza, M., Moore, J., Hendrix, M., 2004. High-resolution particle size analysis of naturally occurring very fine-grained sediment through laser diffractometry. J. Sed. Res. 74, 736–743.

Van Auken, O.W., 2000. Shrub invasions of North American semiarid grasslands. Annu. Rev. Ecol. Syst. 31, 197–215.

Wainwright, J., 2006. Climate and climatological variations in the Jornada Basin. In: Havstad, K.M., Huenneke, L.F., Schlesinger, W.H. (Eds.), Structure and Function of a Chihuahuan Desert Ecosystem: The Jornada Basin Long-term Ecological Research Site. Oxford University Press, Oxford, New York, pp. 44–80.

Warren, A., Chappell, A., Todd, M.C., Bristow, C., Drake, N., Engelstaedter, S., Martins, V., M'bainayel, S., Washington, R., 2007. Dust-raising in the dustiest place on Earth. Geomorphology 92, 25–37.

Wolfe, S.A., Nickling, W.G., 1993. The protective role of sparse vegetation in wind erosion. Prog. Phys. Geogr. 17, 50–68.

Zender, C.S., Bian, H.S., Newman, D., 2003. Mineral dust entrainment and deposition (DEAD) model: description and 1990s dust climatology. J. Geophys. Res. 108, D14. doi:10.1029/2002JD002775.

Zobeck, T., Amante-Orozco, A., 2001. Effect of dust source clay and carbonate content on fugitive dust emissions. In: Proceedings of the 10th International Emissions Inventory Conference, U.S. Environmental Protection Agency, Denver, CO, May 2001, 13 pp.

Zobeck, T.M., 2004. Rapid soil particle size analyses using laser diffraction. Appl. Eng. Agric. 20, 633–639.